Electron-density and electrostatic-potential features of orthorhombic chlorine trifluoride

A. V. Shishkina, A. I. Stash, B. Civalleri, A. Ellern, V. G. Tsirelson
Electron-density and electrostatic-potential features of orthorhombic chlorine trifluoride.
Mendeleev Communications, 20, 161-164, 2010,
http://dx.doi.org/10.1016/j.mencom.2010.05.013.

Electron-density and electrostatic-potential features of orthorhombic chlorine trifluoride

By Anastasia V. Shishkina[a], Adam I. Stash[a,b], Bartolomeo Civalleri[c], Arkady Ellern[d], Vladimir G. Tsirelson[a]

[a] *Mendeleev University of Chemical Technology, 125047 Moscow, Russian Federation. Tel.:+7-499- 9789584; e-mail: tsirel@muctr.edu.ru*
[b] *Karpov Institute of Physical Chemistry, 103064 Moscow, Russian Federation. Tel.: +7-495- 9163146; e-mail: adam@cc.nifhi.ac.ru*
[c] *Università di Torino and NIS Centre of Excellence, 10125 Torino, Italy. Tel.: +39-011-6707564; e-mail: bartolomeo.civalleri@unito.it*
[d] *Iowa State University, Ames, IA, 50011, USA. Tel.: +1-515-2947956; Fax:+1-515-2945717 e-mail: Ellern@iastate.edu*

The intermolecular interactions in solid ClF_3 are analyzed in terms of the Quantum Theory of Atoms in Molecules and Crystals using experimental and theoretical electron density.

The ClF_3 molecules in a crystal are held together by the van der Waals (vdW) forces, which manifest themselves by the appearance of the electron-density bridges linking the neighboring molecules[1]. The mechanics of intermolecular vdW bonding is the same as that of the closed-shell intramolecular bonding[1a], however, the electron density in the intermolecular space of solid ClF_3 is very small and rather flat. It makes difficult the reconstruction of the electron density from the high-resolution X-ray diffraction data. In addition, ClF_3 is a very strong oxidizing and fluorination agent, which is extremely reactive with most inorganic and organic materials[1c, f, 2]. Also, it is non-flammable in air but supports combustion with almost all organic vapours and liquids. These facts not only result in difficulties in obtaining the stable ClF_3 single-crystal of good diffraction quality but also make its X-ray diffraction study nontrivial[3]. The quantum-chemical determination of tiny intermolecular electron-density bridges meets a similar problem due to the lack of a proper description of the electron correlation in the intermolecular regions[4].

In this report, we describe for the first time the electron-density features of the atomic and molecular interactions in orthorhombic ClF_3 crystal by using the low-temperature experimental X-ray diffraction data[†, ‡] and high-level theoretical[§] computation of a three-dimensional periodical crystal. We also present the electrostatic-potential features revealing the nature of the attractive electrostatic interaction, which exists between the atoms in solid ClF_3 even though they carry the same-sign formal charge. The Quantum Theory of Atoms in Molecules and Crystals (QTAIMC)[5], which provides a basis for a comprehensive description of bonding in molecules and crystals, is applied for these purposes.

---

† Chlorine trifluoride was synthesized according to ref. [6]. Traces of HF were removed by the heating the resulting mixture for 24 hours in monel autoclave over pre-dried in vacuum at 500C NaF. 4-fold trap-to-trap distillation in the monel-stainless steel vacuum system resulted to chromatographically pure sample without traces of HF and ClF_5. Thermal analysis of the sample was in a good agreement with the published data for a melting point of pure ClF_3 of -76.3°C [7]. A thin walled quartz capillary (diam. 0.4 mm) was connected to the vacuum line and ClF_3 was condensed into a several time in order to passivate the glass surface. After that the capillary was pumped under heating (400°C) for 24 hours. A passivated capillary was filled with fresh portion of ClF_3 by vacuum condensation, seeled while frozen and transferred to the X-ray diffractometer without interrupting the cooling process. The single crystal was grown at approximately -80°C by cooling with gradient 5 degrees/hour to crystallize low-temperature orthorhombic modification, which is stable below -83.1°C [3].

Crystallographic data: crystal of ClF_3 is orthorhombic at 153K, space group Pnma, a=8.8101(9), b=6.0995(6), c=4.5145(4) Å, 242.60(4) $Å^3$, Z=4, $\mu(MoK_\alpha)$ = 13.7 cm^{-1}. Intensities of 5646 diffraction reflections (-14<h<17, -11<k<10, -8<l<8; $\sin\theta/\lambda \leq 1.0$ $Å^{-1}$) were measured at 153.0(2) K with CCD-1000 diffractometer [$\lambda(MoK_\alpha)$= 0.71073Å, θ=45.65°]; 879 independent reflections with $I>2\sigma(I)$ was obtained; R_{int} = 0.071. The unit cell parameters were obtained from three series of ω scans at different starting angles. Each series consisted of 30 frames collected at intervals of 0.3º in a 10º range about ω with the exposure time of 5 seconds per frame. The obtained reflections were successfully indexed by an automated indexing routine built in the SMART program.

The data were collected using the full sphere routine by collecting four sets of the low-angle frames with 0.3º scans in ω with an exposure time 5 sec per frame and 3 sets of the high-angle frames with exposure time 30 sec per frame. After the background subtraction, the whole data set was corrected for Lorentz and polarization effects.

The structure of ClF_3 was solved by direct method and refined by the full-matrix least-squares technique against F^2 using the spherical-atom model and the anisotropic harmonic approximation for atomic displacements (R = 0.042, wR = 0.118, GOF = 1.13). The atomic relativistic scattering factors and anomalous scattering corrections were taken from[8]. Isotropic secondary extinction considered according to Becker & Coppens (1974)[9] was found to be negligible. All calculations were performed using SHELXTL (version 5.1) program library[10].

Atomic coordinates, bond lengths, bond angles and thermal parameters have been deposited at the Cambridge Crystallographic Data Centre (CCDC). These data can be obtained free of charge *via* www.ccdc.cam.uk/conts/retrieving.html (or from the CCDC, 12 Union Road, Cambridge CB2 1EZ, UK; fax: +44 1223 336 033; or deposit@ccdc.cam.ac.uk). Any request to the CCDC for data should quote the full literature citation and CCDC reference number 289403. For details, see 'Notice to Authors', *Mendeleev Commun.*, Issue 1, 2008.

‡ The Hansen & Coppens (1978) [11a] multipole structural model at the hexadecupole level (program MOLDOS97/MOLLY [11]) was employed in a refinement based on $|F|$ with weights $w=0.5/[\sigma^2(|F|) + 0.0001F^2]$; 759 independent reflections with $I>3\sigma(I)$ were used: R = 0.024, wR = 0.034, GOF = 1.20. Both core and valence electron shells were described by the atomic many-configuration relativistic wave functions[12]. Anomalous dispersion corrections were taken into account[13]. The atomic displacements were described in the anharmonic approximation using the Gram-Charlier expansion of temperature factor up to the tensors of fourth rank[13]. The significance of the structural model of ClF_3 was checked using the Hamilton[14a] test, which showed that account of anharmonicity, is significant at 0.05 level. The validity of the refinement was also controlled by the Abrahams-Keve (1971)[14b] plot. All the experimental-density-based calculations were done with WinXPRO program[15].

§ Calculations on the ClF_3 crystal have been carried out within the Kohn-Sham formalism at the B3LYP-D* level corresponding to the B3LYP functional augmented with a damped empirical pair-wise correction term (i.e. $-f_{dmp}C_6/R^6$) to include long-range dispersion interactions[16] A development version of the CRYSTAL06 code[17a,b] has been used. The accuracy level was controlled by five values that were set to 7 7 7 7 14. The (75,975)p atomic grid has been used with 75 radial points within the Gauss-Legendre and 975 angular points on the Lebedev surface in the most accurate integration region. The shrinking factor of the commensurate reciprocal-space grid was set to 4, corresponding to 27 independent **k**-vectors in the irreducible Brillouin zone. It was found that tighter parameters affected computed results only marginally; therefore, the accuracy in one- and two-electron integrals calculation, DFT numerical integration and sampling of the reciprocal space was adequate to model the crystalline structure of ClF_3.

A full crystal geometry optimization[17c] was carried out by using analytical energy gradients[17d,e]. Convergence was tested on the rms and the absolute value of the largest component of the gradients and the estimated displacements. The crystal structure optimization was considered complete when the maximum force, the rms force, the maximum atomic displacement, and the rms atomic displacement were simultaneously satisfied to values 0.00045, 0.00030, 0.00180, and 0.00120 a.u., respectively. Vibrational frequencies at the Γ point[Errore. Il segnalibro non è definito.f] were computed through a numerical differentiation of the analytical energy gradients.

Nine different TZ and QZV basis sets from Ahlrichs' family with increasing number of atomic functions were employed ranging from 438 to 800 functions in the unit cell. Details on the basis set choice and discussion of calculations will be published elsewhere[18]. We found that a QZV2P basis set is the minimal choice that leads to the correct crystalline Pnma

phase. It did not show any imaginary frequency and yielded good agreement with X-ray measurements (a=8.720, b=6.239, c=4.525). Then, the multipole refinement was carried out within the Hansen-Coppens formalism[11a] using the structure factors obtained from the QZV2P wave function (1818 independent reflections with $I>3\sigma(I)$, $\sin\theta/\lambda \leq 1.0$ Å^{-1}; R=0.004, wR=0.004, GOF= 1.11). It allowed us to compare the electron-density features derived in the same manner.

The network of the bond paths in electron density[5] reflecting the electron-density (ED) bridges linking both atoms in molecules and the neighboring molecules was revealed (Fig. 1 and Fig. 2). In orthorhombic ClF_3 crystal, the molecules form the layers parallel to the (100) plane. Each layer consists of ribbons along *z* axis with the shortest intermolecular F2-F2 contact of 2.687 Å perpendicular to the (010) plane. The shortest Cl-F1 distance between molecules in the ribbons is 3.421 Å. The Cl-F and F-F distances between the ribbons belonging different layers are in the range from 3.064 to 3.409 Å and from 2.966 to 3.288 Å, respectively. A molecule in a crystal has 14 neighboring molecules; each Cl atom has eight neighboring F atoms while the F atoms have six adjoining atoms. Note that the atomic positional parameters derived in this work agree within one e.s.d. with those derived by the neutron diffraction at the same temperature[2a].

The level of the random error in the experimental ED estimated via e.s.d. in the multipole parameters[19] proved to be 0.04 e·Å^{-3} at the bond critical points (BCP) of the Cl−F1 and Cl−F2 intramolecuar bonds, while between atoms involved in the vdW interactions it is only 0.002 e·Å^{-3}. The ED in the middle of intermolecular distances in ClF_3 varies from 0.02 to 0.06 e·Å^{-3}, well above the error bar. The experimental and theoretical ED parameters of the intra- and intermolecular BCPs in ClF_3, reconstructed via the multipole model, reasonably match each other (see Table 1S in Supporting materials). The Laplacian of electron density, $\nabla^2\rho_b(\mathbf{r})$, is positive (closed-shell interactions) and ranges between molecules from 0.36 to 0.96 e·Å^{-5}. This agrees with the QTAIMC analyses of both theoretical and experimental ED in other vdW molecular systems[1a, c, f-i], which show the flat distribution of electron density in the intermolecular regions with $\rho_b(\mathbf{r}) \sim 0.02\text{-}0.07$ e·Å^{-3} and $\nabla^2\rho_b(\mathbf{r}) \sim +(0.20\text{-}0.85)$ e·Å^{-5}. The atomic basins in the electron density (ρ-basins) limited by the surfaces S defined by the condition $\nabla\rho(\mathbf{r})\cdot\mathbf{n}(\mathbf{r}) = 0$, where $\mathbf{n}(\mathbf{r})$ is a unit vector normal to the surface S at $\mathbf{r}$ showed the aspheric shapes (Fig. 2) and comparable sizes (Table 2S). Because these volumes are proportional to the atomic polarizabilities and reflect the additive contributions to the molecular polarizability[20a], it can be supposed that all the atoms yield the comparable contributions to the dispersion interaction of molecules in a crystalline ClF_3. The atomic electron populations computed by integration of experimental and theoretical ED within the atomic ρ-basins allowed to determine the atomic charges, which are given in Table 2S. They show that atom F2 carries the higher negative net charge.

The dipole-dipole molecular interactions define the general packing motif in the crystalline ClF_3, while the tiny packing details can be described in terms of the molecular recognition[1i,20]. The latter is due to the intermolecular vdW interactions and may be interpreted by using the concept of molecular complementarity. It shows two limiting cases: the first, a van der Waals complementarity, is determined by the size and shape of contacting atoms or atomic groups; the second, a Lewis complementarity, is responsible of the assembly of the molecules by adjustment of their electrophilic and nucleophilic ("acid and base") molecular sites. Analysis of the Laplacian of the electron density, $\nabla^2\rho(\mathbf{r})$, allows to distinguish these cases [1i, 20b, c]. The peaks of local concentrations in valence-shell ED, where $\nabla^2\rho(\mathbf{r})<0$, indicate the nucleophilic molecular sites, while the local areas of the valence-shell ED depletion (the "holes" where $\nabla^2\rho(\mathbf{r}) > 0$), locate the electrophilic activity sites. The Lewis complementary corresponds to fitting of lumps and holes in adjacent molecules as observed for solid Cl_2[1c], ClF[1f], S_4N_4[1h], N_2O_4[1i], C_6Cl_6[21a] and As_2O_5, AsO_2, As_2O_3 [21b]. In contrast, a van der Waals complementarity does not exhibit the evident peak-to-hole fitting of adjacent molecules and the specificity of its mechanism is not established yet in detail.

To establish which type of molecular complementarity dominates in orthorhombic ClF_3, the Laplacians of experimental and theoretical EDs were computed (see Fig. 2 and Fig. 1S, 2S in Supporting Materials). The maps displaying the areas of function $\nabla^2\rho < 0$ superimposed with the bond paths in ClF_3 show that the concentrations in the valence-shell ED as appeared in the function $\nabla^2\rho(\mathbf{r})$ form the tori around the F atoms (see the inserts in Fig. 2), no noticeable peaks were found. In contrast, the well localized $-\nabla^2\rho(\mathbf{r})$ peaks in the valence shells of Cl atoms are present and can be associated with the electron lone pairs. However these peaks do not lead to the peak-to-hole fitting in adjacent molecules. Thus Fig. 2 and Fig. 1S, 2S allow to conclude that a van der Waals complementarity dominates in orthorhombic ClF_3.

We can speculate that the absence of the evident peak-to-hole interactions can be related to the small values in the electron density bridges between ClF_3 molecules reflecting the weak bond directivity of the intermolecular F-F and F-Cl contacts in solid ClF_3.

To understand the features of the electrostatic contributions to the atom-atom interactions in ClF_3, we have considered the inner-crystal electrostatic field, $\mathbf{E}(\mathbf{r}) = -\nabla\varphi(\mathbf{r})$ where $\varphi(\mathbf{r})$ is electrostatic potential (ESP). The field $\mathbf{E}(\mathbf{r})$ defines the classic inner-crystal electrostatic force $\mathbf{F}(\mathbf{r})= q\ \mathbf{E}(\mathbf{r})$ acting on the charge q at point $\mathbf{r}$. Nuclei of neighboring atoms in any crystal are separated in the electric fields $\mathbf{E}(\mathbf{r})$ and $\mathbf{F}(\mathbf{r})$ by surfaces P_i, satisfying the zero-flux condition $\mathbf{E}(\mathbf{r})\cdot\mathbf{n}(\mathbf{r}) = \mathbf{F}(\mathbf{r})\cdot\mathbf{n}(\mathbf{r}) = 0$, $\forall\mathbf{r} \in P_i(\mathbf{r})$;

n(**r**) is a unit vector normal to the surface P_i at **r**. Each surface P_i defines the φ-basin of i-*th* atom, inside of which the electrons are attracted to the nuclei *i* [22]. The $\nabla\varphi(\mathbf{r})$ gradient field allows us to highlight the network of the atomic-like φ-basins in solid ClF_3 (Fig. 3). Also, it allows revealing the network of atomic electrostatic interactions in this crystal. Indeed, because the electron density within each φ-basin is attracted to the corresponding nucleus, the overlap of the ρ-basins and φ-basins of adjacent atoms A and B leads to situation in which the part of the ED belonging to A atom falls into φ-basin of B atom (Fig. 4). In solid ClF_3, the ρ-basins of F1 and F2 atom overlap the φ-basins of Cl atom both within each molecule and between the neighbouring molecules (Cl-F contacts numbering as I, II, III, IV, IX – see Table 1S). The same applies to the contact F2-F1 (V). That provides the physical basis for electrostatic atom-atom attraction in ClF_3 crystal. It also explains why the attractive electrostatic interaction exists between the atoms in solid ClF_3 even though they carry the same-sign formal net charge.

We have to note that the formation of the intermolecular bond paths in electron density is not always accompanied by the overlap of the atomic ρ-basins and φ-basins. For example, the boundaries of the ρ-basin and φ-basin of F2-F2 atoms lined by the bond path (contact VII) exactly coincide (Fig. 4). In general, electrostatic-interaction picture does not exhibit the directional character and does not link with the bond paths in the electron density, which are related with quantum effects.

Thus, this work has allowed us to clarify the complete picture of the intermolecular interactions in orthorhombic ClF_3. It was found that a van der Waals complementarity dominates in solid ClF_3; it is determined by the size and shape of contacting atoms and does not show the adjustment of neighboring molecules by means of fitting localized valence-shell charge concentrations and depletions. Partial overlap of atomic-like basins created by zero-flux surfaces in both the electron density and the electrostatic potential is an origin of the attractive electrostatic interaction between atoms in solid ClF_3 even though they carry the same-sign formal charge.

AVS, AIS and VGT acknowledge the Russian Foundation for Basic Research, grant № 07-03-00702.

References

1 (a) R. G. A. Bone, R. F. W. Bader, *J. Phys. Chem.*, 1996, **B100,** 10892; (b) R. F. W. Bader, *J. Phys. Chem.*, 1998, **A102,** 7314; (c) V. G. Tsirelson, P. F. Zou, T. H. Tang, R. F. W. Bader, *Acta Crystallogr.*, 1995, **A51,** 143; (d) J. Hernańdez-Trujillo, R. F. W. Bader, *J. Phys. Chem.*, 2000, **A104,** 1779; (e) R. F. W. Bader, J. Hernańdez-Trujillo, F. Corteś-Guzmań, *J. Comput. Chem.*, 2007, **28,** 4; (f) R. Boese, A. D. Boese, D. Blaser, M. Yu. Antipin, A. Ellern, K. Seppelt, *Angew. Chem., Int. Ed. Engl.*, 1997, **36,** 1489; (g) R. Boese, D. Blaser, O. Heinemann, Yu. Abramov, V. G. Tsirelson, P. Blaha, K. Schwarz, *J. Phys. Chem.*, 1999, **A103,** 6209; (h) W. Scherer, M. Spiegler, B. Pedersen, M. Tafipolsky,

W. Hieringer, B. Reinhard, A. J. Downs, G. S. McGrady, *Chem. Commun.*, 2000, **7,** 635; (i) V. G. Tsirelson, A. V. Shishkina, A. I. Stash, S. Parsons., *Acta Crystallogr.*, 2009, **B65,** 647.
2 (a) R. D. Burbank, F. N. Bensey, *J. Chem. Phys*., 1953, **21**, 602; (b) A. J. Edawards, R. J. C. Sills, *J. Chem. Soc.* **A**, 1970, 2697; (c) G. Skirrow, H. G. Wolfhard, *Proc. R. Soc. Lond*., 1955, **A232**, 78; (d) A. P. Taylor, B. Fruhberger, R. Hogle (1999), **7** (http://www.semiconductor.net).
3 M. Yu. Antipin, A. M. Ellern, V. F. Sukhoverkhov, Yu. T. Struchkov, *Russ. Journ. Inorg. Chem.*, 1989, **34**, 459.
4 Y. Zhao, D. G. Truhlar, *Acc. Chem. Res.*, 2008, **41**, 157.
5 R. F. W. Bader, In Atoms in Molecules: A Quantum Theory, J. Halpen, M.L.H. Green, Eds.;
6 The International Series of Monographs of Chemistry; Clarendon Press: Oxford, 1990.
7 O. Ruff, H. Krug, *Z. Anorg. Allg. Chem*., 1930, **190**, 270.
http://encyclopediaairliquidecom
8 A. J. C. Wilson, Ed., International Tables for Crystallography, v. C; Kluwer Academic Publishers: Dordrecht, 1995.
9 P. J. Becker, P. Coppens, *Acta Crystallogr.*, 1974, **A30**, 129.
10 (a) G. M. Sheldrick, *Acta Crystallogr.*, 2008, **A64**, 112–122; (b) G. Sheldrick, Bruker Analytical X-Ray Systems, Madison, WI.
11 (a) N. K. Hansen, P. Coppens, *Acta Crystallogr.*, 1978, **A34**, 909; (b) J. Protas, 1997, MOLDOS97/ MOLLY IBM PC-DOS.
12 P. Macchi & P. Coppens, 2001, *Acta Cryst* A**57**, 656.
13 International Tables for Crystallography, v. C; A. J. C. Wilson, Ed.; Kluwer Academic Publishers: Dordrecht, 1995.
14 (a)W. C. Hamilton, *Acta Crystallogr*., 1965, **18**, 502; (b) S. C. Abrahams, E.T. Keve, *Acta Crystallogr.*, 1971, **A27**, 157.
15 (a) A. I. Stash, V. G. Tsirelson, *J. Appl. Crystallogr*., 2002, **35**, 371; (b) A. I. Stash, V. G. Tsirelson, *Crystallogr. Rep.*, 2005, **50**, 202.
16 S. Grimme, *J. Comp. Chem.*, 2006, **27**, 1787.
17 (a) R. Dovesi, V. R. Saunders, C. Roetti, R. Orlando, C. M. Zicovich-Wilson, F. Pascale, B. Civalleri, K. Doll, N. M. Harrison, I. J. Bush, P. D'Arco, M. Llunell, *CRYSTAL06 User's Manual*; Universita` di Torino: Torino, 2006; (b) B. Civalleri, C. M. Zicovich-Wilson, L. Valenzano, P. Ugliengo, *CrystEngComm*, 2008, **10**, 405; (c) B. Civalleri, P. D'Arco, R. Orlando, V. R. Saunders, R. Dovesi, *Chem. Phys. Lett.*, 2001, **348**, 131; (d) K. Doll, V. R. Saunders, N. M. Harrison, *Int. J. Quantum Chem.*, 2001, **82**, 1; (e) K. Doll, R. Dovesi, R. Orlando, *Theor. Chem. Acc.*, 2004, **112**, 394; (f) F. Pascale, C. M. Zicovich-Wilson, F. L. Gejo, B. Civalleri, R. Orlando, R. Dovesi, *J. Comp. Chem.*, 2004, **25**, 888.
18 B. Civalleri, A. V. Shishkina, A. I. Stash, V. G. Tsirelson, *J. Mol. Struct. (THEOCHEM)*, 2009, submitted.
19 V. G. Tsirelson, R. P. Ozerov, *Electron Density and Bonding in Crystals* Bristol, England/ Philadelphia, USA: Institute of Physics Publishing, 1996.
20 (a) R. F. W. Bader, T. A. Keith, K. M. Gough, K. E. Laidig, *Mol. Phys.*, 1992, **75,** 1167; (b) C. F. Matta, R. F. W. Bader, *Proteins*, 2003, **52**, 360; (c) R. F. W. Bader, P. J. MacDougall, C. D. H. Lau, *J. Am. Chem. Soc.*, 1984, **106**, 1594–1605.
21 (a) T. T. T. Bui, S. Dahaoui, C. Lecomte, G. R. Desiraju, E. Espinosa, *Angew. Chem. Int. Ed.*, 2009, **48**, 3838; (b) G. V. Gibbs, A. F. Wallace, D. F. Cox, P. M. Dove, R. T. Downs, N. L. Ross, K. M. Rosso., *J. Phys. Chem.*, 2009, **A113**, 736.
22 V. G. Tsirelson, A. S. Avilov, G. G. Lepeshov, A. K. Kulygin, J. Stahn, U. Pietsch, J. C. H. Spence, *J. Phys. Chem.*, 2001, **B105**, 5068.

Figure captures to the paper by Shishkina et al

Figure 1. The molecular structure of orthorhombic crystal ClF_3.

Figure 2. The distribution of Laplacian of electron density in the plane A: (a) the model electron-density was derived from the X-ray diffraction experiment; (b) B3LYP/QZV2P/model calculation. Only positive Laplacian values are shown; the line intervals are 2×10^n, 4×10^n and 8×10^n e $Å^{-5}$ ($-2 \leq n \leq 2$). The sections of Laplacian in the planes going through F1 and F2 atoms perpendicular to the Cl-F1 and Cl-F2 lines are also given as the inserts. The critical points (3,-1) and (3,+1) in electron density are marked by the red points and blue triangles.

Figure 3. The inner-crystal vector electric field in the plane A (see Fig 2) in the unit cell of solid ClF_3 (experiment);

Figure 4. The superposition of interatomic surfaces of ρ-basins and φ –basins in the plane A (the B3LYP/QZV2P/model calculation). The intramolecular bond paths are shown by the thin black lines, while the intermolecular bond paths are indicated by the black dashed lines. The interatomic surface of ρ-basins is marked by solid black lines, φ –basins of Cl, F1 and F2 atoms are depicted over white, bright grey and dark grey colour correspondently. The critical points (3,-1) in electron density are shown by the red points.

Figure 1.

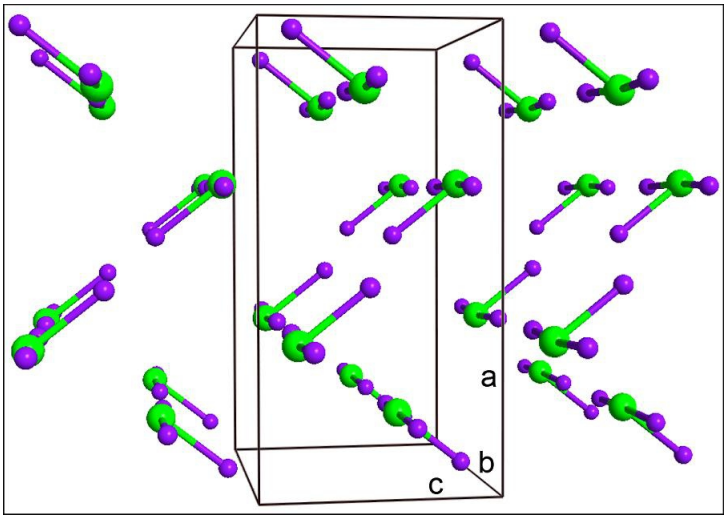

Figure 2.

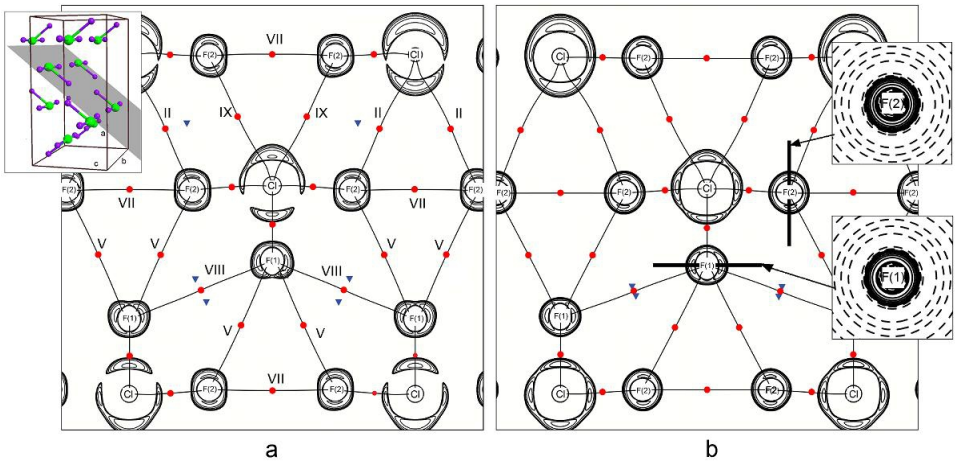

Figure 3.

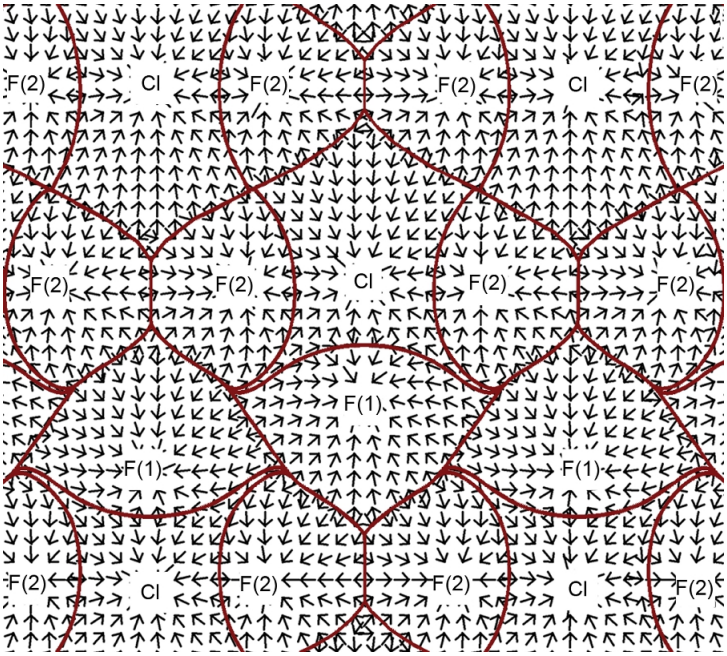

Figure 4.